# Phase Equilibria of Haloalkanes Dissolved in Ethylsulfate- or Ethylsulfonate-Based Ionic Liquids

**Francisco J. Deive,[†,‡] Ana Rodríguez,[‡] Ana B. Pereiro,[†,‡] Karina Shimizu,[†,§] Paulo A. S. Forte,[†] Carlos C. Romão,[†] José N. Canongia Lopes,*[,†,§] José M. S. S. Esperança,*[,†] and Luís P. N. Rebelo[†]**

*Instituto de Tecnologia Química e Biológica, UNL, Avenida República 127, 2780-901 Oeiras, Portugal, Chemical Engineering Department, University of Vigo, 36310, Vigo, Spain, and Centro de Química Estrutural, Instituto Superior Técnico, UTL, 1049 001 Lisboa, Portugal*

*Received: March 19, 2010; Revised Manuscript Received: April 22, 2010*

The temperature−composition phase diagrams of 40 binary mixtures composed of a haloalkane dissolved in either 1-ethyl-3-methylimidazolium ethylsulfate or 1-ethyl-3-methylimidazolium ethylsulfonate were measured from ambient temperature to the boiling point temperature of the solute. The coexistence curves corresponding to liquid−liquid equilibria (LLE) boundaries were visually determined and the experimental results have been correlated using either the nonrandom two-liquid (NRTL) model or a set of empirical equations capable of describing the corresponding upper critical solution temperatures (UCSTs) loci. The different types of LLE behavior were discussed in terms of the type of ionic liquid solvent, the alkyl-chain length of the solute, and the type and pattern of halogen substitution present in the haloalkane. Auxiliary simulation data (obtained by ab initio or by molecular dynamics methods) were used to corroborate some of the experimental findings. Also, they correlate in a semiquantitative way the observed LLE behavior with the dipole moments of the different solutes.

## Introduction

Because of some of their unique properties,[1−4] namely, their almost null vapor pressure, general nonflammability and thermal stability, ionic liquids are commonly considered a "cleaner" alternative to traditional volatile organic compounds in the implementation of new separation techniques.[5] In this context, liquid−liquid equilibria (LLE) data are essential for the correct development and optimization of such processes.

Ionic liquids based on the alkylsulfate anion combined with dialkylimidazolium cations are considered promising salts in terms of possible industrial applications;[6] in general, they are easily synthesized in an atom-efficient and halide-free way, at a reasonable cost. As a result, several LLE studies involving mixtures containing 1-ethyl-3-methylimidazolium ethylsulfate, [$C_2$mim][$EtSO_4$], have been published.[7,8] In contrast, and despite its much better thermal stability,[9] no analogous studies dealing with 1-ethyl-3-methylimidazolium ethylsulfonate, [$C_2$mim][$EtSO_3$], were found.

This work focuses on the differences between the solvent quality toward selected solutes of those two ionic liquids, which differ (slightly) on the nature of their constituting anions (ethylsulfate versus ethylsulfonate). The solutes are all mono- or disubstituted haloalkanes, $C_mH_{2m+1}X$ or $C_nH_{2n}X_2$, where X = Br or Cl and $m$ varies from 3 to 7 for the monosubstituted compounds and $n$ is 3 or 4 for the disubstituted ones. These solutes were chosen because (i) they have a sufficiently large liquid range superimposed to that of the ionic liquids (all solutes are liquid at room temperature and have an adequately high normal boiling point temperature, in the 350−400 K range in most cases); (ii) they all show liquid−liquid immiscibility windows with the selected ionic liquids; and (iii) two of the factors that influence the LLE behavior can be tailored into the solute molecule, the size of the nonpolar moiety of the molecule and the intensity of its dipolar moment. The latter is influenced by the nature, amount, and position of the halogen substitution (chlorine versus bromine, single versus double, primary carbon versus secondary carbon substitutions).

## Experimental Section

**Chemicals.** The haloalkane compounds were supplied by (a) Sigma Aldrich, 1-bromopropane (99% mass fraction), 1,3-dibromopropane (99% mass fraction), 1-bromobutane (99% mass fraction), 1,2-dibromobutane (97% mass fraction), 1,3-dibromobutane (97% mass fraction), 1-bromoheptane (99% mass fraction), 1-chloropropane (98% mass fraction), 1,2-dichloropropane (99% mass fraction), 1-chlorobutane (99% mass fraction), 1,2-dichlorobutane (98% mass fraction), 1,3-dichlorobutane (99% mass fraction), 1-chloropentane (99% mass fraction), 1-chlorohexane (99% mass fraction), and 1-chloroheptane (99% mass fraction); (b) by Alfa Aesar, 1,2-dibromopropane (98% mass fraction), 1,4-dibromobutane (99% mass fraction), 1-bromohexane (98% mass fraction), 1,3-dichloropropane (95% mass fraction), and 1,4-dichlorobutane (97% mass fraction); and (c) by Fluka, 1-bromopentane (98.5% mass fraction). These chemicals were used without further treatment.

[$C_2$mim][$EtSO_4$] was purchased from Solvent Innovation (99% stated purity). [$C_2$mim][$EtSO_3$] was prepared according to a previously described procedure.[9,10] To reduce the water and other volatile substances contents, vacuum ($10^{-1}$ Pa) and moderate temperature (ca. 320 K) were always applied to all samples of both ionic liquids for several hours prior to their use. After degassing, the purity was checked by H NMR. The

* To whom correspondence should be addressed. E-mail: (J.N.C.L.) jnlopes@ist.utl.pt; (J.M.S.S.E.) jmesp@itqb.unl.pt.
† Instituto de Tecnologia Química e Biológica, UNL, www.itqb.unl.pt.
‡ University of Vigo.
§ Instituto Superior Técnico, UTL, cqe.ist.utl.pt.

10.1021/jp1025015 
Published on Web 05/06/2010

$^1$H spectra confirmed purity levels higher or around 99%. The final water mass fraction was measured by Karl Fischer coulometric titration (Metrohm 831 KF Coulometer). The dried samples contained less than 150 ppm of water for both ionic liquids.

**Experimental Procedure.** All cloud-point determinations, plotted herein as temperature−composition LLE phase diagrams at atmospheric pressure, were performed using a visual detection of the solution's turbidity. For this purpose, Pyrex glass cells equipped with magnetic stirrers were used. Solutions were gravimetrically prepared directly inside the cells using an analytical high-precision balance with an uncertainty of ±0.01 mg. The cells were then immersed in a thermostatic bath and the samples inside them were continuously stirred up to the occurrence of the phase transition. A water−ethylene glycol bath was used for measurements between room temperature and 333 K. Measurements at higher temperature (from 333 to 430 K) were performed using a silicone oil bath. The temperature of the liquid−liquid phase transition (cloud-point temperature) was taken at the point in which the first sign of turbidity appeared in the homogeneous solution upon cooling. Data were then confirmed by repeated cooling−heating cycles (three in most cases). Temperatures were measured using a four-wire platinum resistance thermometer coupled to a Yokogawa 7561 multimeter. The temperature uncertainty in both baths was ±0.01 K and the estimated uncertainty of the mixtures composition was $\pm 10^{-4}$ in mole fraction.

**Simulation.** The molecular force field used to represent the ionic liquids and the haloalkane solutes is based on the OPLS-AA model[11] but with parameters specifically tailored in the case of the ionic liquid ions.[12,13] Following the spirit of OPLS-AA, intramolecular terms related to covalent bonds and angles were taken from the AMBER force field,[14] and efforts were concentrated on carefully describing conformational and intermolecular terms. Therefore, special attention has been paid to obtaining torsion energy profiles and electrostatic charge distributions, using ab initio calculations with a high level of theory (MP2 method) and large basis sets (cc-pVTZ(-f)), performed using the Gaussian03 program package.[15]

Six solutions of 1-chloropropane, 1,2-dichloropropane, and 1,2-dibromopropane either in [$C_2$mim][$EtSO_3$] or in [$C_2$mim]-[$EtSO_4$] were studied at 300 K. All simulations were performed using molecular dynamics, implemented in the DL_POLY code.[16] Starting from low-density initial configurations, systems composed of 250 ion pairs were equilibrated at constant *NpT* for 500 ps at 300 K (Nosé-Hoover thermostat and barostat with time constants of 0.5 and 2 ps, respectively). The final density was attained after about 50 ps. Further simulation runs of 100 ps were used to produce equilibrated systems at the studied temperatures. Electrostatic interactions were treated using the Ewald summation method considering 6 reciprocal-space vectors, and repulsive-dispersive interactions were explicitly cut off at 1.6 nm (long-range corrections were applied assuming the system had an uniform density beyond this cutoff radius). Then, 1000 configurations were stored from production runs of 300 ps, in order to obtain statistical meaningful radial distribution functions between selected atom pairs.

## Results

The phase diagrams depicting liquid−liquid immiscibility windows in binary mixtures of different haloalkanes ($C_mH_{2m+1}X$) or ($C_nH_{2n}X_2$) in [$C_2$mim][$EtSO_3$] or [$C_2$mim]-[$EtSO_4$] ionic liquids, where X stands for either bromide or chloride and $3 \leq m \leq 7$ and $3 \leq n \leq 4$, were experimentally determined from 298 K to close to the normal boiling point temperature of each haloalkane solute. The experimental phase diagrams are shown in Figures 1 to 6. Tables 1 to 4 contain the corresponding LLE data.

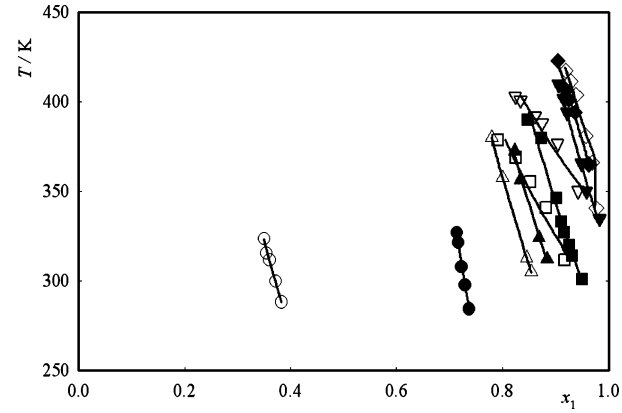


**Figure 1.** Effect of alkyl side-chain length on the $T-x$ phase diagrams (LLE boundaries; two-phase regions to the left of respective lines) of ionic liquid (1) + 1-bromoalkanes (2) systems. Full and void symbols represent [$C_2$mim][$EtSO_4$] and [$C_2$mim][$EtSO_3$], respectively: (○, ●), 1-bromopropane; (△, ▲), 1-bromobutane; (□, ■), 1-bromopentane; (▽, ▼), 1-bromohexane; (◇, ◆), 1-bromoheptane. Solid lines represent data fits to eq 1.

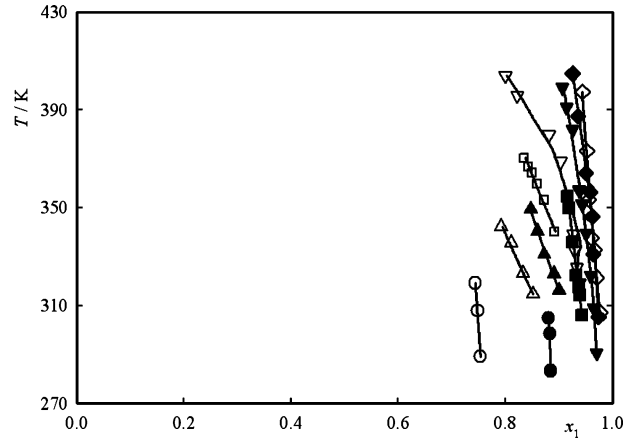


**Figure 2.** Effect of alkyl side-chain length on the $T-x$ phase diagrams (LLE boundaries; two-phase regions to the left of respective lines) of ionic liquid (1) + 1-chloroalkanes (2) systems: (○, ●), 1-chloropropane; (△, ▲), 1-chlorobutane; (□, ■), 1-chloropentane; (▽, ▼), 1-chlorohexane; (◇, ◆), 1-chloroheptane. Full and void symbols as well as solid lines as in Figure 1.

Figures 1 and 2 show the influence of the alkyl chain length of the bromo- and chloro-monosubstituted alkanes on the demixing behavior of the mixtures. In general terms, miscibility is lower for (i) the sulfate-based solvents as compared to the sulfonate ones, (ii) longer alkyl-side chains on the haloalkane, and (iii) the chloride-based (short-chained) solutes as compared to the bromide ones. For these monosubstituted solutes, the immiscibility regions exhibit similar topologies, almost null solubility of both ionic liquids in the pure haloalkanes (as tested by the addition of a single nonmiscible drop), finite solubilities, increasing with increasing temperature, of the haloalkane in the ionic liquid ranging from 5 to 30% in solute mole fraction (except for bromopropane in [$C_2$mim][$EtSO_3$], which shows a solubility of about 60%), and the absence of any locus corresponding to an upper critical solution temperature within the working temperature range.

The experimental LLE data for the twenty binary systems containing monosubstituted alkanes were correlated using the

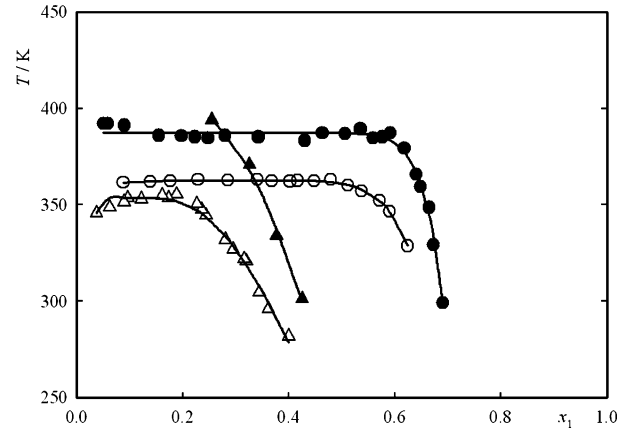


**Figure 3.** Effect of halogen relative position on the $T-x$ phase diagrams (LLE boundaries; two-phase regions to the left and below of respective lines) of ionic liquid (1) + dibromoalkanes (2) systems: (○, ●), 1,2-dibromopropane; (Δ, ▲), 1,3-dibromopropane. Full and void symbols as in Figure 1. Solid lines represent data fits to eq 2.

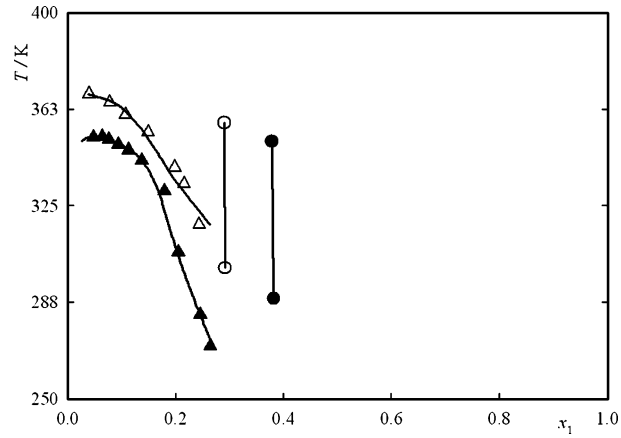


**Figure 4.** Effect of halogen relative position on the $T-x$ phase diagrams (LLE boundaries; two-phase regions to the left and below of respective lines) of ionic liquid (1) + dichloroalkanes (2) systems: (○, ●), 1,2-dichloropropane; (Δ, ▲), 1,3-dichloropropane. Full and void symbols as well as solid lines as in Figure 1.

nonrandom two-liquid (NRTL) equation (cf. ESI) with temperature-dependent interaction parameters,[17] $\Delta g_{ij}$, defined as

$$\Delta g_{ij} = a_{ij} + b_{ij}T/\mathrm{K} + c_{ij}\ln(T/\mathrm{K}) \qquad (1)$$

The three fitting parameters $a_{ij}$, $b_{ij}$, and $c_{ij}$ and the temperature-independent NRTL nonrandomness parameter α were estimated by minimizing the deviations between the calculated and experimental compositions at the liquid−liquid immiscibility boundary curves for each system as a function of temperature. The results obtained are reported in Table 5, along with the root-mean-square deviations of each fitted curve, $\sigma$. The adequacy of the fitting procedure can be attested by the small deviations found in this case (below 2%) and also by the fitting curves represented in Figures 1 and 2.

Figures 3 to 6 depict the immiscibility envelopes of mixtures of different dihalopropane or dihalobutane solutes dissolved in sulfate- or sulfonate-based ionic liquids. Generally speaking, solubility continues to be lower for the sulfate-based ionic liquids and for longer alkyl chains (butane-based versus propane-based solutes), but unlike the monosubstituted alkanes, the dibromoalkanes tend to be less soluble than their chlorinated counterparts. Moreover, most disubstituted haloalkanes exhibit

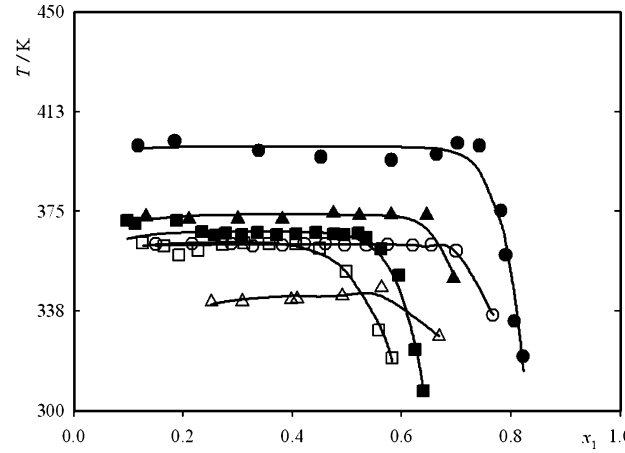


**Figure 5.** Effect of halogen relative position on the $T-x$ phase diagrams (LLE boundaries; two-phase regions to the left and below of respective lines) of ionic liquid (1) + dibromoalkanes (2) systems: (○, ●), 1,2-dibromobutane; (Δ, ▲), 1,3-dibromobutane; (□, ■), 1,4-dibromobutane. Full and void symbols, and solid lines as in Figure 3.

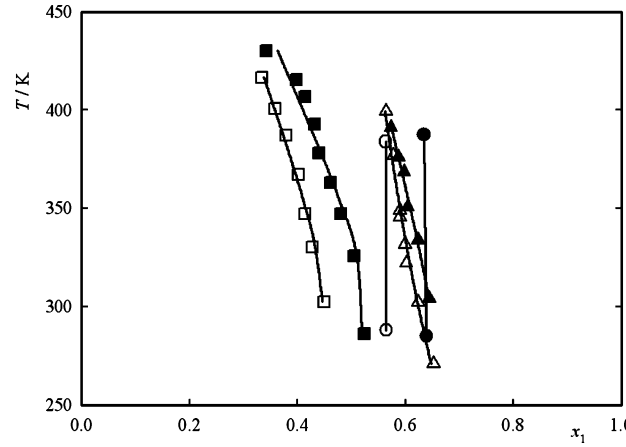


**Figure 6.** Effect of halogen relative position on the $T-x$ phase diagrams (LLE boundaries; two-phase regions to the left of respective lines) of ionic liquid (1) + dichloroalkanes (2) systems: (○, ●), 1,2-dichlorobutane; (Δ, ▲), 1,3-dichlorobutane; (□, ■), 1,4-dichlorobutane. Full and void symbols as well as solid lines as in Figure 1.

larger solubilities than their monosubstituted counterparts with many LLE envelopes showing the existence of upper critical solution loci, especially in the case of dibromoalkane solutes. The relative position of the two halogen atoms in the solute also affects the LLE equilibria with adjacent-disubstituted solutes (1,2-dihaloalkanes) exhibiting lower solubilities than 1,3- or 1,4-dihaloalkanes. Most binary systems involving dihaloalkane solutes exhibit immiscibility envelopes with upper critical solution temperatures (UCST). In this case the data were fitted to the equations[18]

$$T = T_c + k|y - y_c|^n \quad (y = \alpha x/(1 + x(\alpha\text{-}1))) \qquad (2)$$

where $n$, $k$, α, $T_c$, and $x_c$ are fitting parameters with the last two representing the temperature and composition of the UCST, respectively. Results are collected in Table 6 and plotted in Figures 3−6. It should be noted that due to the extreme flatness of the upper consolute temperature envelopes, the uncertainty in the critical composition is so high that excludes any possible discussion based on this variable.[19,20]

**TABLE 1: Experimental LLE Data for the Binary Mixtures [$C_2$mim][$EtSO_4$] (1) + Bromoalkanes (2)**

| *T*/K | $x_1$ | *T*/K | $x_1$ | *T*/K | $x_1$ | *T*/K | $x_1$ |
|---|---|---|---|---|---|---|---|
| **1-$C_3H_7Br$** | | **1-$C_7H_{15}Br$** | | **1,3-$C_3H_6Br_2$** | | **1,4-$C_4H_8Br_2$** | |
| 284.22 | 0.7371 | 365.04 | 0.9633 | 301.09 | 301.09 | 307.42 | 0.6389 |
| 297.41 | 0.7292 | 393.99 | 0.9365 | 333.96 | 333.96 | 322.95 | 0.6246 |
| 307.80 | 0.7228 | 401.22 | 0.9253 | 370.89 | 370.89 | 350.92 | 0.5955 |
| 321.27 | 0.7165 | 406.62 | 0.9192 | 394.05 | 394.05 | 360.82 | 0.5626 |
| 326.71 | 0.7135 | 422.77 | 0.9042 | **1,2-$C_4H_8Br_2$** | | 365.18 | 0.5360 |
| **1-$C_4H_9Br$** | | **1,2-$C_3H_6Br_2$** | | 320.38 | 0.8228 | 366.80 | 0.5208 |
| 312.24 | 0.8841 | 299.21 | 0.6913 | 333.65 | 0.8067 | 366.18 | 0.4951 |
| 324.15 | 0.8687 | 329.30 | 0.6728 | 358.62 | 0.7906 | 366.41 | 0.4761 |
| 356.48 | 0.8338 | 348.65 | 0.6649 | 375.18 | 0.7817 | 366.99 | 0.4432 |
| 372.54 | 0.8228 | 359.47 | 0.6481 | 399.69 | 0.7423 | 366.35 | 0.4069 |
| **1-$C_5H_{11}Br$** | | 365.73 | 0.6408 | 400.62 | 0.7023 | 366.12 | 0.3709 |
| 300.90 | 0.9497 | 379.20 | 0.6183 | 396.41 | 0.6642 | 366.95 | 0.3360 |
| 314.04 | 0.9313 | 387.37 | 0.5920 | 394.29 | 0.5813 | 366.10 | 0.3079 |
| 319.97 | 0.9252 | 385.19 | 0.5772 | 395.42 | 0.4521 | 366.88 | 0.2786 |
| 327.30 | 0.9164 | 384.47 | 0.5589 | 397.91 | 0.3382 | 366.05 | 0.2569 |
| 333.17 | 0.9103 | 389.29 | 0.5356 | 401.54 | 0.1848 | 367.21 | 0.2349 |
| 346.16 | 0.9011 | 386.84 | 0.5064 | 399.69 | 0.1180 | 371.55 | 0.1881 |
| 379.64 | 0.8719 | 387.13 | 0.4635 | **1,3-$C_4H_8Br_2$** | | 370.49 | 0.1131 |
| 389.79 | 0.8468 | 383.25 | 0.4308 | 349.79 | 0.6951 | 371.45 | 0.0981 |
| **1-$C_6H_{13}Br$** | | 385.19 | 0.3429 | 373.56 | 0.6459 | | |
| 334.74 | 0.9827 | 385.95 | 0.2801 | 373.68 | 0.5810 | | |
| 349.93 | 0.9580 | 384.71 | 0.2478 | 373.39 | 0.5223 | | |
| 365.43 | 0.9490 | 385.19 | 0.2226 | 374.17 | 0.4747 | | |
| 393.82 | 0.9220 | 385.68 | 0.1976 | 372.04 | 0.3814 | | |
| 401.78 | 0.9149 | 385.92 | 0.1554 | 372.15 | 0.3003 | | |
| 409.53 | 0.9060 | 391.20 | 0.0899 | 372.07 | 0.2106 | | |
| | | 392.06 | 0.0590 | 373.00 | 0.1322 | | |
| | | 392.06 | 0.0506 | | | | |

**TABLE 2: Experimental LLE Data for the Binary Mixtures [$C_2$mim][$EtSO_3$] (1) + Bromoalkanes (2)**

| *T*/K | $x_1$ | *T*/K | $x_1$ | *T*/K | $x_1$ | *T*/K | $x_1$ |
|---|---|---|---|---|---|---|---|
| **1-$C_3H_7Br$** | | **1-$C_7H_{15}B$** | | **1,3-$C_3H_6Br_2$** | | **1,4-$C_4H_8Br_2$** | |
| 288.03 | 0.3826 | 340.47 | 0.9767 | 281.73 | 0.3996 | 319.87 | 0.5827 |
| 299.54 | 0.3717 | 366.05 | 0.9694 | 296.07 | 0.3614 | 330.35 | 0.5583 |
| 311.42 | 0.3605 | 380.81 | 0.9571 | 304.51 | 0.3443 | 352.29 | 0.4987 |
| 315.30 | 0.3546 | 403.53 | 0.9389 | 320.87 | 0.3195 | 360.98 | 0.4493 |
| 323.24 | 0.3500 | 411.20 | 0.9285 | 321.98 | 0.3161 | 362.87 | 0.4068 |
| **1-$C_4H_9Br$** | | 417.28 | 0.9195 | 326.96 | 0.2950 | 362.72 | 0.3576 |
| 304.83 | 0.8508 | **1,2-$C_3H_6Br_2$** | | 331.96 | 0.2802 | 362.98 | 0.3114 |
| 312.85 | 0.8474 | 328.74 | 0.6244 | 344.53 | 0.2435 | 362.49 | 0.2728 |
| 357.49 | 0.8059 | 346.58 | 0.5909 | 347.50 | 0.2356 | 360.29 | 0.2278 |
| 379.97 | 0.7752 | 352.29 | 0.5711 | 350.56 | 0.2268 | 358.59 | 0.1931 |
| **1-$C_5H_{11}Br$** | | 357.00 | 0.5369 | 355.30 | 0.1881 | 361.87 | 0.1658 |
| 311.34 | 0.9174 | 360.00 | 0.5115 | 353.65 | 0.1728 | 363.05 | 0.1264 |
| 340.77 | 0.8816 | 363.05 | 0.4795 | 354.89 | 0.1608 | **1,2-$C_4H_8Br_2$** | |
| 355.30 | 0.8516 | 362.41 | 0.4477 | 352.92 | 0.1218 | 336.00 | 0.7670 |
| 368.54 | 0.8248 | 362.58 | 0.4166 | 353.44 | 0.0963 | 360.08 | 0.6999 |
| 378.55 | 0.7909 | 362.20 | 0.4024 | 351.49 | 0.0889 | 362.40 | 0.6540 |
| **1-$C_6H_{13}Br$** | | 362.46 | 0.3677 | 348.51 | 0.0623 | 362.15 | 0.6202 |
| 350.10 | 0.9431 | 363.16 | 0.3406 | 345.79 | 0.0372 | 362.53 | 0.5744 |
| 376.64 | 0.9038 | 362.62 | 0.2857 | **1,3-$C_4H_8Br_2$** | | 362.15 | 0.5359 |
| 388.10 | 0.8748 | 363.18 | 0.2290 | 327.92 | 0.6682 | 362.40 | 0.4955 |
| 391.87 | 0.8614 | 362.45 | 0.1765 | 346.30 | 0.5635 | 362.75 | 0.4610 |
| 400.85 | 0.8334 | 361.91 | 0.1384 | 343.20 | 0.4917 | 362.83 | 0.4219 |
| 402.98 | 0.8240 | 361.64 | 0.0879 | 342.08 | 0.4085 | 362.22 | 0.3819 |
| | | | | 341.86 | 0.3981 | 362.00 | 0.3281 |
| | | | | 341.09 | 0.3082 | 362.91 | 0.2892 |
| | | | | 340.91 | 0.2521 | 362.88 | 0.2166 |
| | | | | | | 362.65 | 0.1504 |

The simulation trajectories in the six solutions of 1-chloropropane, 1,2-dichloropropane, and 1,2-dibromopropane either in [$C_2$mim][$EtSO_3$] or in [$C_2$mim][$EtSO_4$] were used to calculate the corresponding radial pair distribution functions between selected pairs of interaction centers. These structural data were used to corroborate some of the conclusions inferred from the solubility results and are discussed in the following section (see below).

## Discussion

Table 7 shows the comparison of the solubility data for the forty studied systems at an average temperature of 330 K, calculated from interpolations (or small extrapolations) of the fitting equations.

The compilation of LLE data on forty distinct systems has allowed us to discuss five different issues that affect the mutual

**TABLE 3: Experimental LLE Data for the Binary Mixtures [$C_2$mim][$EtSO_4$] (1) + Chloroalkanes (2)**

| $T$/K | $x_1$ | $T$/K | $x_1$ | $T$/K | $x_1$ | $T$/K | $x_1$ |
|---|---|---|---|---|---|---|---|
| **1-$C_3H_7Cl$** | | **1-$C_6H_{13}Cl$** | | **1,2-$C_3H_6Cl_2$** | | **1,3-$C_4H_8Cl_2$** | |
| 283.33 | 0.8847 | 290.65 | 0.9703 | 289.12 | 0.3812 | 304.05 | 0.6437 |
| 298.52 | 0.8830 | 308.81 | 0.9649 | 350.00 | 0.3780 | 333.81 | 0.6236 |
| 304.96 | 0.8804 | 322.17 | 0.9593 | **1,3-$C_3H_6Cl_2$** | | 350.92 | 0.6040 |
| **1-$C_4H_9Cl$** | | 339.51 | 0.9512 | 270.65 | 0.2638 | 368.44 | 0.5973 |
| 316.13 | 0.9002 | 351.34 | 0.9441 | 282.78 | 0.2455 | 375.97 | 0.5869 |
| 323.03 | 0.8909 | 357.31 | 0.9388 | 307.11 | 0.2052 | 391.20 | 0.5727 |
| 331.01 | 0.8724 | 357.00 | 0.9386 | 330.68 | 0.1785 | **1,4-$C_4H_8Cl_2$** | |
| 340.48 | 0.8603 | 381.89 | 0.9255 | 342.68 | 0.1365 | 286.04 | 0.5233 |
| 349.49 | 0.8472 | 390.96 | 0.9145 | 346.74 | 0.1122 | 325.67 | 0.5050 |
| **1-$C_5H_{11}Cl$** | | 399.03 | 0.9067 | 348.79 | 0.0935 | 347.37 | 0.4801 |
| 306.15 | 0.9433 | **1-$C_7H_{15}Cl$** | | 350.87 | 0.0760 | 362.91 | 0.4621 |
| 314.20 | 0.9390 | 305.39 | 0.9740 | 351.93 | 0.0643 | 378.36 | 0.4400 |
| 317.56 | 0.9375 | 330.96 | 0.9641 | 351.57 | 0.0473 | 392.87 | 0.4313 |
| 322.46 | 0.9327 | 346.45 | 0.9621 | 350.23 | 0.0391 | 406.82 | 0.4139 |
| 335.87 | 0.9259 | 356.48 | 0.9591 | **1,2-$C_4H_8Cl_2$** | | 415.55 | 0.3983 |
| 350.02 | 0.9192 | 364.22 | 0.9507 | 285.10 | 0.6387 | 430.34 | 0.3428 |
| 354.72 | 0.9166 | 387.37 | 0.9358 | 387.40 | 0.6344 | | |
| | | 404.77 | 0.9255 | | | | |

**TABLE 4: Experimental LLE Data for the Binary Mixtures [$C_2$mim][$EtSO_3$] (1) + Chloroalkanes (2)**

| $T$/K | $x_1$ | $T$/K | $x_1$ | $T$/K | $x_1$ | $T$/K | $x_1$ |
|---|---|---|---|---|---|---|---|
| **1-$C_3H_7Cl$** | | **1-$C_6H_{13}Cl$** | | **1,2-$C_3H_6Cl_2$** | | **1,3-$C_4H_8Cl_2$** | |
| 289.18 | 0.7534 | 319.10 | 0.9385 | 301.00 | 0.2914 | 270.87 | 0.6523 |
| 307.92 | 0.7483 | 325.45 | 0.9337 | 357.30 | 0.2900 | 302.14 | 0.6236 |
| 319.26 | 0.7435 | 332.52 | 0.9294 | **1,3-$C_3H_6Cl_2$** | | 322.16 | 0.6015 |
| **1-$C_4H_9Cl$** | | 339.05 | 0.9268 | 317.74 | 0.2434 | 331.83 | 0.5996 |
| 314.75 | 0.8512 | 368.87 | 0.9035 | 333.65 | 0.2149 | 348.97 | 0.5901 |
| 323.28 | 0.8330 | 379.98 | 0.8818 | 339.96 | 0.1976 | 345.76 | 0.5898 |
| 335.69 | 0.8111 | 395.80 | 0.8223 | 353.64 | 0.1486 | 377.02 | 0.5780 |
| 342.30 | 0.7920 | 404.05 | 0.7997 | 360.40 | 0.1073 | 399.56 | 0.5637 |
| **1-$C_5H_{11}Cl$** | | **1-$C_7H_{15}Cl$** | | 365.22 | 0.0777 | **1,4-$C_4H_8Cl_2$** | |
| 340.33 | 0.8911 | 307.16 | 0.9774 | 368.44 | 0.0391 | 302.50 | 0.4493 |
| 353.19 | 0.8725 | 321.51 | 0.9713 | **1,2-$C_4H_8Cl_2$** | | 347.29 | 0.4136 |
| 359.73 | 0.8590 | 332.88 | 0.9670 | 288.00 | 0.5645 | 330.18 | 0.4278 |
| 364.29 | 0.8499 | 337.74 | 0.9605 | 384.00 | 0.5634 | 367.21 | 0.4015 |
| 366.66 | 0.8430 | 353.38 | 0.9562 | | | 387.13 | 0.3782 |
| 370.52 | 0.8349 | 373.26 | 0.9526 | | | 400.73 | 0.3583 |
| | | 397.43 | 0.9443 | | | 416.73 | 0.3338 |

solubility of the two components of the binary mixtures, (i) solvent effect (sulfate- versus sulfonate-based ionic liquids); (ii) solute alkyl-chain size (from C3 to C7 in monohaloalkanes, C3 versus C4 in dihaloalkanes); (iii) halogen type (bromoalkanes versus chloroalkanes); (iv) amount of substitution (mono- versus dihaloalkanes); and (v) relative positions of substitution (1,2-, 1,3-, or 1,4-dihaloalkanes).

(i) The difference between the sulfonate-based and sulfate-based ionic liquid solvents can be, obviously, attributed to the presence of the extra oxygen bridge-atom in the sulfate anion. This atom, placed between the charged $SO_3$ group and the nonpolar alkyl side chain, causes shifts in the charge distribution of the anion especially in the first carbon atom of the alkyl side chain (cf. Table 1 of ref 13 and Figure 7). Despite their structural similarities, the ethylsulfate and ethylsulfonate anions are in fact quite different with the former exhibiting a larger polar moiety and the possibility of forming more extensive polar networks when combined with different cations. This means that dipolar aprotic solutes like the haloalkanes studied in this work will have more difficulty in dissolving in the tightly bound [$C_2$mim][$EtSO_4$] than in the less bound [$C_2$mim][$EtSO_3$]. The results presented in Table 7 corroborate this fact; the solubility of all solutes is lower in the sulfate-based ionic liquid than in its sulfonate counterpart, except in the case of 1,3-dichloropropane (discussed below).

(ii) The concept of ionic liquids as nanosegregated media[26] can also explain at a molecular level their solvation properties toward different classes of solutes.[27] This concept states that ionic liquids exhibit medium-range ordering, that is, there are persistent microscopic heterogeneities in the liquid phase. These heterogeneities correspond to polar domains, composed of the high-charge density head groups of the ions, and to nonpolar regions, composed of the low-charge density alkyl side chains of those same ions. The latter regions can accommodate nonpolar solutes, while the former can interact strongly with dipolar or associative solutes.[28] In the present case both ionic liquids have very short alkyl side chains (the ends of the two ethyl groups of the anion and the cation) attached to their polar head groups (the sulfate and sulfonate groups of the anions and the imidazolium ring and adjacent atoms of the cation), that is, their nonpolar regions are very small. This means that haloalkanes with progressively larger alkyl groups will have more difficulty in being solvated by the (almost exclusively polar) ionic liquid. Again, Table 7 shows this effect for all haloalkane solutes, irrespective of their mono or disubstituion.

(iii) The effects of chlorine versus bromine substitution are subtler than what one could anticipate based on just the size and electronegativity differences between the chlorine and bromine atoms. In fact 1-bromoalkanes and 1-chloroalkanes exhibit almost identical dipole moments in the gas phase and

**TABLE 5: Fitting Parameters and Root-Mean-Square Deviation, $\sigma$, of the NRTL Model Used to Correlate the LLE Experimental Data Containing 1-Haloalkane and Dichloroalkane Solutes[a]**

| System | $a_{21}$ J·mol$^{-1}$ | $b_{21}$ J·K$^{-1}$·mol$^{-1}$ | $c_{21}$ J·mol$^{-1}$ | α | $\sigma$ |
|---|---|---|---|---|---|
| [$C_2$mim][$EtSO_4$](1) | | | | | |
| 1-$C_3H_7Br$ (2) | 14.36 | 0.898 | −0.778 | 0.64 | 0.001 |
| [1-$C_4H_9Br$ (2) | 14.38 | 0.891 | −0.792 | 0.61 | 0.003 |
| 1-$C_5H_{11}Br$ (2) | 13.95 | 0.862 | −0.718 | 0.60 | 0.007 |
| 1-$C_6H_{13}Br$ (2) | 13.95 | 0.862 | −0.696 | 0.60 | 0.004 |
| 1-$C_7H_{15}Br$ (2) | 23.71 | 0.990 | −2.397 | 0.60 | 0.003 |
| 1-$C_3H_7Cl$ (2) | 13.89 | 0.887 | −0.608 | 0.63 | 0.001 |
| 1,2-$C_3H_6Cl_2$ (2) | 21.53 | 1.024 | −2.070 | 0.69 | 0.001 |
| 1,3-$C_3H_6Cl_2$ (2) | 17.84 | 0.963 | −1.757 | 0.42 | 0.046 |
| 1-$C_4H_9Cl$ (2) | 14.89 | 0.903 | −0.916 | 0.58 | 0.003 |
| 1,2-$C_4H_8Cl_2$ (2) | 13.36 | 0.867 | −0.551 | 0.65 | 0.001 |
| 1,3-$C_4H_8Cl_2$ (2) | 18.85 | 0.983 | −1.562 | 0.65 | 0.006 |
| 1,3-$C_4H_8Cl_2$ (2) | 28.60 | 1.094 | −3.265 | 0.67 | 0.039 |
| 1-$C_5H_{11}Cl$ (2) | 13.73 | 0.857 | −0.616 | 0.62 | 0.001 |
| 1-$C_6H_{13}Cl$ (2) | 18.39 | 0.927 | −1.364 | 0.62 | 0.002 |
| 1-$C_7H_{15}Cl$ (2) | 17.87 | 0.874 | −1.460 | 0.59 | 0.010 |
| [$C_2$mim][$EtSO_3$](1) | | | | | |
| 1-$C_3H_7Br$ (2) | 14.67 | 0.906 | −1.068 | 0.63 | 0.004 |
| 1-$C_4H_9Br$ (2) | 14.38 | 0.891 | −0.800 | 0.61 | 0.007 |
| 1-$C_5H_{11}Br$ (2) | 14.41 | 0.872 | −0.870 | 0.53 | 0.017 |
| 1-$C_6H_{13}Br$ (2) | 15.42 | 0.890 | −1.040 | 0.49 | 0.015 |
| 1-$C_7H_{15}Br$ (2) | 20.73 | 0.937 | −1.919 | 0.59 | 0.004 |
| 1-$C_3H_7Cl$ (2) | 13.09 | 0.871 | −0.537 | 0.64 | 0.001 |
| 1,2-$C_3H_6Cl_2$ (2) | 28.25 | 1.157 | −3.268 | 0.72 | 0.001 |
| 1,3-$C_3H_6Cl_2$ (2) | 37.42 | 1.497 | −5.110 | 0.49 | 0.097 |
| 1-$C_4H_9Cl$ (2) | 15.21 | 0.910 | −1.019 | 0.55 | 0.004 |
| 1,2-$C_4H_8Cl_2$ (2) | 30.73 | 1.230 | −3.543 | 0.66 | 0.001 |
| 1,3-$C_4H_8Cl_2$ (2) | 11.06 | 0.951 | −0.386 | 0.48 | 0.008 |
| 1,3-$C_4H_8Cl_2$ (2) | 26.82 | 1.121 | −2.990 | 0.68 | 0.014 |
| 1-$C_5H_{11}Cl$ (2) | 14.38 | 0.873 | −0.870 | 0.51 | 0.004 |
| 1-$C_6H_{13}Cl$ (2) | 34.32 | 0.927 | −4.068 | 0.63 | 0.012 |
| 1-$C_7H_{15}Cl$ (2) | 16.34 | 0.779 | −1.188 | 0.59 | 0.016 |

[a] For all systems $a_{12} = 11.00$ J·mol$^{-1}$, $b_{12} = 2222$ J·K$^{-1}$·mol$^{-1}$, and $c_{12} = 12.00$ J·mol$^{-1}$.

**TABLE 6: Parameters and Root-Mean-Square Deviation, $\sigma$, of the UCST Adjustment Equations Used to Correlate the Experimental Data Containing Dibromoalkane Solutes[a]**

| | $n$ | α | $T_c$/K | $x_{1c}$ | $\sigma$ |
|---|---|---|---|---|---|
| [$C_2$mim][$EtSO_4$] (1) | | | | | |
| 1,2-$C_3H_6Br_2$ | 139.45 | 10.452 | 387.47 | 0.001 | 2.782 |
| 1,3-$C_3H_6Br_2$ | 6.84 | 9.440 | 405.56 | 0.091 | 2.240 |
| 1,2-$C_4H_8Br_2$ | 7.77 | 0.564 | 399.40 | 0.432 | 5.209 |
| 1,3-$C_4H_8Br_2$ | 5.43 | 0.321 | 373.87 | 0.427 | 2.037 |
| 1,4-$C_4H_8Br_2$ | 5.09 | 0.427 | 367.33 | 0.340 | 4.159 |
| [$C_2$mim][$EtSO_3$] (1) | | | | | |
| 1,2-$C_3H_6Br_2$ | 4.06 | 0.189 | 362.74 | 0.330 | 0.496 |
| 1,3-$C_3H_6Br_2$ | 6.22 | 12.159 | 353.72 | 0.093 | 2.412 |
| 1,2-$C_4H_8Br_2$ | 6.49 | 0.287 | 362.60 | 0.444 | 0.337 |
| 1,3-$C_4H_8Br_2$ | 3.74 | 0.142 | 343.45 | 0.481 | 1.488 |
| 1,4-$C_4H_8Br_2$ | 2.83 | 0.089 | 363.46 | 0.289 | 1.180 |

[a] For all systems $k$ was assumed to be −67095. $T_c$ and $x_{1c}$ are the critical temperature and critical composition (mole fraction of ionic liquid), respectively.

in different solvents (around 2 D ≡ $6.7 \times 10^{-30}$ C·m in nonpolar solvents like benzene or tetrachloromethane).[22] The substituted end of the haloalkane (where the dipolar charge separation is concentrated, Figure 8) is responsible for most of the interactions with the high-charge density parts of the ionic liquids ions, with the rest of the haloalkane (the alkyl side chain) acting as a residue that has to be "tolerated" by the ionic liquid solvent (that in this case does not have any nanosegregated nonpolar regions in its midst, cf. above). This explains the already discussed lower solubility of the longer 1-haloalkanes and also the fact that those (low) solubilities are almost the same irrespective of the type of halogen substitution, although the 1-bromoalkanes tend to be slightly more soluble (cf. Figures 1 and 2, where the lines with open symbols are always to the left of the corresponding lines with filled symbols). Only in the case of 1-bromopropane and 1-chloropropane there are significant differences in the solubility of these solutes in the two studied ionic liquids with the former 1-haloalkane exhibiting larger solubility values, especially in the [$C_2$mim][$EtSO_3$] solvent. Given the similarity of the dipole moment of the two molecules it is hard to interpret such large differences. However, it is known that solutes that are able to maintain simultaneously strong interactions with both ions of an ionic liquid exhibit enhanced solubility. This is the case of small strongly dipolar molecules like acetone or acetonitrile, but also strongly quadrupolar molecules such as carbon dioxide, benzene, or perfluorinated benzene.[27,29,30] In the present case, 1-bromopropane and 1-chloropropane do not have to accommodate a long alkyl side chain. This means that, released from that extra burden, the solute capable of interacting simultaneously with the cation (interactions between the halogen and the hydrogen atoms of the imidazolium ring) and the anion (interactions between the substituted carbon atom of the haloalkane and the oxygen atoms of the anions) exhibit a larger solubility in the ionic liquid, cf. simulated structural data in the form of radial distribution functions presented in Figure 9. Apparently, 1-bromopropane accomplishes that task more efficiently than 1-chloropropane, especially in the sulfonate-based ionic liquid that has the ions not so tightly connected in its polar network (see above), and, therefore, allows for the simultaneous interaction of the solute with parts of that network. In this context, the larger polarizability of the bromine atom certainly plays a role in promoting more efficient, flexible and dual interactions with both ions of the ionic liquid.

(iv) and (v) When one changes from monosubstituted to disubstituted haloalkane solutes one might expect that the solubility in ionic liquids should increase; after all, two halogen−carbon dipolar bonds should work better than just one. In fact, solubility does increase but a lot of other issues should be also taken into account such as dichloroalkane solutes are more soluble than dibromoalkane ones, the relative position of the substitution (1,2 versus 1,3 versus 1,4) has a huge effect on the solubility, and in some cases the solubility dramatically increases with increasing temperature leading to the appearance of UCST behavior associated with the LLE.

The first issue that must be addressed is that the dipole moments of dihaloalkanes are not necessarily larger than those of monohaloalkanes. The reason is quite straightforward; if the substituton takes place in different carbon atoms (as in the studied cases of 1,2-, 1,3-, and 1−4-dihaloalkanes) the molecule can use its internal rotation to adopt several conformations in which the relative positions of the two halogen atoms yield quite different molecular dipole moments, including some with an almost null value, corresponding to opposite ("transoid") configurations of the two halogen atoms. In the case of 1,2-dihaloalkanes the role of stereochemical hindrance and hyperconjugation is also not negligible (especially in the case of 1,2-dibromoalkanes) leading to conformers that are much more stable than others and that do not interconvert very easily. Table 7 shows the values of molecular dipole moment for the different haloalkane solutes studied in this work. These values must be understood as the overall average of several contributions from different molecular conformations resulting from the more or less hindered internal rotation of the molecules.

**TABLE 7: Dipole Moments at Room Temperature, $\mu$, and Solubility Limits at 330 K of Haloalkane Solutes in Sulfonate- or Sulfate-Based Ionic Liquids (Expressed in Mole Fractions of Solvent)**

| | $\mu$ (Debye) | | solubility (solvent mole fraction) | | | |
|---|---|---|---|---|---|---|
| solvent | $C_6H_6$ or $CCl_4$[a] | | $[C_2mim][EtSO_3]$ | | $[C_2mim][EtSO_4]$ | |
| solute | X = Br | X = Cl | X = Br | X = Cl | X = Br | X = Cl |
| 1-$C_3H_7X$ | 1.95[b] | 2.0[c] | 0.3435 | 0.7405 | 0.7114 | 0.8756 |
| 1-$C_4H_9X$ | 1.96[b] | 2.0[c] | 0.8274 | 0.8192 | 0.8634 | 0.8770 |
| 1-$C_5H_{11}X$ | 1.96[d] | | 0.8897 | 0.9153 | 0.9148 | 0.9298 |
| 1-$C_6H_{13}X$ | 1.96[d] | 2.0[c] | 1.0000 | 0.9373 | 0.9845 | 0.9559 |
| 1-$C_7H_{14}X$ | | | 0.9809 | 0.9670 | 0.9899 | 0.9676 |
| 1,2-$C_3H_6X_2$ | 1.13[e] | 1.46[e] | 0.6228 | 0.2905 | 0.6752 | 0.3790 |
| 1,3-$C_3H_6X_2$ | 1.99[f] | 2.07[f] | 0.2864 | 0.2154 | 0.3832 | 0.1710 |
| 1,2-$C_4H_8X_2$ | | | 0.7739 | 0.5640 | 0.8150 | 0.6380 |
| 1,3-$C_4H_8X_2$ | | | 0.6634 | 0.6026 | 0.7202 | 0.6249 |
| 1,4-$C_4H_8X_2$ | 1.96[f] | 2.01[f] | 0.5635 | 0.4328 | 0.6189 | 0.5061 |

[a] The dipole moments of mono- and disubstituted haloalkanes were measured in diluted $C_6H_6$ and $CCl_4$ solutions, respectively. [b] Reference 21. [c] Reference 22. [d] Reference 23. [e] Reference 24. [f] Reference 25.

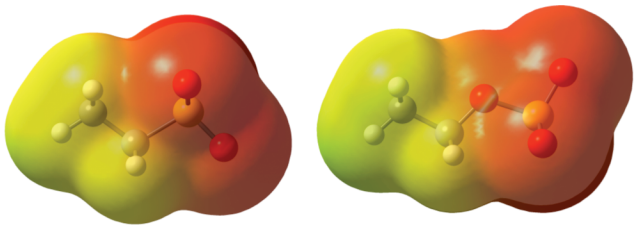

**Figure 7.** Electrostatic potential mapped onto an electron density isosurface around the ethylsulfonate (left) and ethylsulfate (right) anions. The negatively charged regions of the anions are indicated by color gradients ranging from red (strongly negative) to yellow-green (slightly negative−neutral).

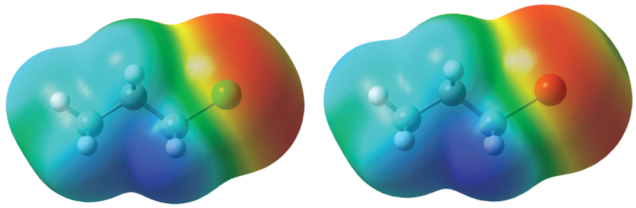

**Figure 8.** Electrostatic potential mapped onto an electron density isosurface around the 1-chloropropane (left) and 1-bromopropane (right) molecules. The positively and negatively charged regions of the molecule are indicated by color gradients ranging from dark blue (strongly positive) to red (strogly negative), Cyan−green−yellow correspond to slightly positive−neutral−slightly negative regions.

The different solubility trends found for the dihaloalkanes can be rationalized taking into account three simple notions [(a)−(c), see below)] that can be inferred from the data contained in Table 7, and, in addition, from both the investigations that originated the dipole moment results[21−25] and the already discussed issue of simultaneous solute-ion dual interactions.

(a) Dichloroalkanes are more soluble than dibromoalkanes (at lower temperatures) because the molecules substituted with the smaller chlorine atoms have less hindered conformations[24] and therefore are able to be more flexible in their interactions with the ions, that is, the larger size and polarizability of the bromine atom, which was an asset in the case of 1-bromoalkanes, is a liability in the case dibromoalkanes due to hindered molecular flexibility (rotation). The polarizability of one bromine atom is traded-off by the enhanced mobility of two chloride atoms. This can be seen by the differences between the molecular dipole moments of analogous chloro- and bromoalkanes. We have seen that the difference is almost null in the case of 1-haloalkanes (both have a value of about 2 D). In the case of 1,2-dibromopropane ($\mu$ =1.13 D in $CCl_4$ at 298 K) and 1,2-dichloropropane ($\mu$ = 1.46 D in the same conditions),[24] the difference is 0.33 D. This does not mean that the dipole moment associated to each individual C−Br bond is smaller, just that the 1,2-dibromomolecule due to the bulkier bromine atoms is "stuck" more often in transoid positions, a fact that obviously hinders its capability to interact in a simultaneous and flexible way with the ions of the ionic liquid.

(b) As the distance between the substituted halogen atoms increases from 1,2- to 1,3- to 1,4- substitutions, two factors concur to yield higher solubilities. On the one hand, substitutions at both ends of the n-alkane chain do not "leave exposed" nonpolar alkyl segments that are always difficult to accommodate in these particular ionic liquid solvents. On the other hand, halogen atoms substituted further apart are less hindered by each other and can adopt different conformations in a more independent way, leading to more effective interactions with the ions of the solvent. This is also the reason why there are huge solubility differences between 1,2-dibromoalkanes (very hindered, see above) and 1,2-dichloroalkanes (still hindered but less so) that are less prominent in the cases of 1,3- or 1,4-substituted solutes. This can be corroborated by checking the dipole moments of 1,2- and 1,3-dichloropropane in $CCl_4$ at 298 K, 1.46 and 2.07 D, respectively.[24,25] It must be stressed that albeit the latter value is almost the same as that of monosubstituted alkanes, the solubility of 1,3-dichloropropane is larger than that of 1-chloropropane due to the added intensity and flexibility conferred by the presence of two (almost independent) C−Cl dipoles.

(c) The final concept is related to the existence of UCSTs in the LLE envelopes of most dibromoalkane systems. It was found[31] that the stability differences and interconversion barriers between the different conformers of dihaloalkanes are progressively overcome as temperature is increased. For instance, the dipole moments of 1,2-dichloropropane in benzene increase from 1.45 to 1.68 D in the 343 to 508 K temperature interval.[32] The effect is expected to be even larger in the case of dibromoalkanes. In other words, the hindrance at lower temperature of the different conformers of the dibromoalkanes can be attenuated at higher temperatures, allowing the true effectiveness of the bromine atoms (through their larger polarizability as compared to that of the chlorine atoms) to play its role in the solvation of the solute molecules. This abrupt change in the internal rotation of the dibromoalkane molecules explains the ubiquitous appearance of UCSTs in the corresponding dibromoalkane plus ionic liquid systems.

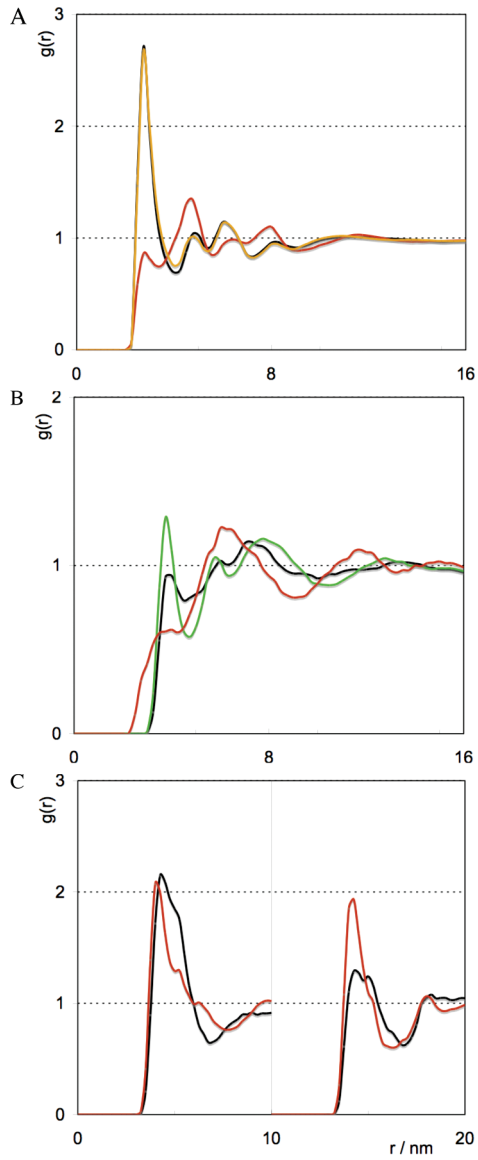


**Figure 9.** Selected pair radial distribution functions (RDFs) of simulated mixtures of 1-chloropropane in [$C_2$mim][$EtSO_4$] and [$C_2$mim][$EtSO_3$] ionic liquids (ILs). Panel A, the IL polar network: RDFs between the most acidic hydrogen atom of the imidazolium ring ($H_R$) and the oxygen atoms of sulfonate ($-SO_3$) (in black) and sulfate ($-OSO_3$ and $-OSO_3$) (orange and red, respectively). The RDFs show that the tightly polar network is stabilized mainly via hydrogen-bonds between $H_R$ and $-OSO_3$; panel B, the IL-solute polar interactions: RDFs between $H_R$ and Cl (red), and between $-OSO_3$ and $C_1$ (green) and $C_3$ (black) of the solute. The RDFs show that the solute-anion interactions (mainly at $C_1$) are stronger than the solute-cation ones; panel C, IL-solute nonpolar interactions: RDFs between $C_1$ (black) and $C_3$ (red) of the solute and the end atom of the ethyl chain in the cation (CEc), on the left, or the anion (CEa), on the right. The RDFs show that the alkyl part of the solute is more easily accommodated near the cation side chain than near the ethyl group of the anions.

A final comment on the solubility of the two systems involving the 1,3-dichloropropane solute is warranted at this stage. Interestingly, and unlike all other systems, this solute exhibits a larger solubility in the sulfate-based ionic liquid than in the sulfonate-based one. Accidentally, this is also the solute that at low temperatures shows larger solubility limits in both ionic liquids (0.83 and 0.79 mol fraction of solute) as compared to any other solute. Taking into account the three types of concept discussed in the previous paragraphs, it is not hard to explain why this is the "best" solute: shortest alkyl chain (propane) with the two smallest halogens (chlorine) substituted as far apart as possible (1,3 substitution). Unfortunately, this particular solute has the lowest quality (purity) among all used haloalkanes. In any case, one is tented to speculate that at a certain point the interactions with the ions of the ionic liquid become so efficient that the solute is able to reap a larger energetic reward by breaking into the more tightly bound sulfate-based ionic liquid, to the detriment of the sulfonate-based one.

## Conclusions

The selection of the solutes to perform this work was based on the assumption that, by careful choice of molecules of distinct dipolar nature, one could obtain different types and ranges of liquid−liquid immiscibility windows. This was a concept that had been previously tested in the case of ionic liquid plus fluorinated benzene mixtures,[30] where the solubility in [$C_2$mim][$NTf_2$] of different aromatic solutes was correlated in a quite striking manner with their dipole and quadrupole moments. Molecular dynamics simulations performed at that time showed at a molecular level the reasons for such strong correlation; the multipolar nature of the aromatic molecules was acting as a charge template for the (re)distribution of the ions of the polar network around the molecular solutes.

The present results have shown a similar trend with the strongly dipolar carbon−halogen bonds acting as the main driving force toward an improved solubility of the haloalkane solute in the ionic liquid by providing the above-mentioned charge template. The results have also shown that other unforeseen factors such as the internal rotation of the dihalogenalkane compounds (a hot topic during the middle of the twentieth century, also rationalized in terms of dipole moments!) can play a crucial role in the development (and rationalization) of unexpected behavior such as the ubiquitous appearance of UCSTs in the dibromoalkane solutions.

**Acknowledgment.** The authors acknowledge Fundação para a Ciência e Tecnologia (FCT/MCTES) through Project PTDC/CTM/73850/2006. J.M.S.S.E. thanks FCT/MCTES for a research contract under the program Ciência 2007. F.J.D. wishes to thank Fundación Juana de Vega for a postdoctoral grant. K.S. acknowledges post-doc FCT grant SFRH/BPD/38339/2007.

**Supporting Information Available:** Description of NRTL equation fitting procedure given as ESI. This material is available free of charge via the Internet at http://pubs.acs.org.

## References and Notes

(1) Earle, M. J.; Esperança, J. M. S. S.; Gilea, M. A.; Canongia Lopes, J. N.; Rebelo, L. P. N.; Magee, J. W.; Seddon, K. R.; Widegren, J. A. The distillation and volatility of ionic liquids. *Nature* **2006**, *439*, 831–834.

(2) Rebelo, L. P. N.; Canongia Lopes, J. N.; Esperança, J. M. S. S.; Filipe, E. On the critical temperature, normal boiling point, and vapor pressure of ionic liquids. *J. Phys. Chem. B* **2005**, *109*, 6040–6043.

(3) Smiglak, M.; Reichert, W. M.; Holbrey, J. D.; Wilkes, J. S.; Sun, L. Y.; Thrasher, J. S.; Kirichenko, K.; Singh, S.; Katritzky, A. R.; Rogers, R. D. Combustible ionic liquids by design: Is laboratory safety another ionic liquid myth. *Chem. Commun.* **2006**, 2554–2556.

(4) Baranyai, K. J.; Deacon, G. B.; MacFarlane, D. R.; Pringle, J. M.; Scott, J. L. Thermal degradation of ionic liquids at elevated temperatures. *Aust. J. Chem.* **2004**, *57*, 145–147.

(5) Seddon, K. R. Ionic liquids for clean technology. *J. Chem. Technol. Biotechnol.* **1997**, *68*, 351–356.

(6) Holbrey, J. D.; Reichert, W. M.; Swatloski, R. P.; Broker, G. A.; Pitner, W. R.; Seddon, K. R.; Rogers, R. D. Efficient, halide free synthesis of new, low cost ionic liquids1,3-dialkylimidazolium salts containing methyl- and ethyl-sulfate anions. *Green Chem.* **2002**, *4*, 407–413.

(7) Domańska, U.; Laskowska, M.; Marciniak, A. Phase Equilibria of (1-Ethyl-3-methylimidazolium Ethylsulfate + Hydrocarbon, + Ketone, and + Ether) Binary Systems. *J. Chem. Eng. Data* **2008**, *53*, 498–502.

(8) Domańska, U.; Laskowska, M. Phase Equilibria and Volumetric Properties of (1-Ethyl-3-Methylimidazolium Ethylsulfate + Alcohol or Water) Binary Systems. *J. Solution Chem.* **2008**, *37*, 1271–1287.

(9) Blesic, M.; Swadzba-Kwasny, M.; Belhocine, T.; Nimal Gunaratne, H. Q.; Canongia Lopes, J. N.; Costa Gomes, M. F.; Pádua, A. A. H.; Seddon, K. R.; Rebelo, L. P. N. 1-Alkyl-3-methylimidazolium alkanesulfonate ionic liquids, $[C_nH_{2n+1}mim][C_kH_{2k+1}SO_3]$: synthesis and physicochemical properties. *Phys. Chem. Chem. Phys.* **2009**, *11*, 8939–8948.

(10) Blesic, M.; Swadzba-Kwasny, M.; Holbrey, J. D.; Canongia Lopes, J. N.; Seddon, K. R.; Rebelo, L. P. N. New catanionic surfactants based on 1-alkyl-3-methylimidazolium alkylsulfonates, $[C_{(n)}H_{(2n+1)}mim]$ $[C_mH_{2m+1}SO_3]$: mesomorphism and aggregation. *Phys. Chem. Chem. Phys.* **2009**, *11*, 4260–4268.

(11) Jorgensen, W. L.; Maxwell, D. S.; Tirado-Rives, J. Development and testing of the OPLS all-atom force field on conformational energetics and properties of organic liquids. *J. Am. Chem. Soc.* **1996**, *118*, 11225–11236.

(12) Canongia Lopes, J. N.; Deschamps, J.; Pádua, A. A. H. Modeling ionic liquids using a systematic all-atom force field. *J. Phys. Chem. B* **2004**, *108*, 2038–2047.

(13) Canongia Lopes, J. N.; Pádua, A. A. H.; Shimizu, K. Molecular force field for ionic liquids IV: Trialkylimidazolium and alkoxycarbonylimidazolium cations; alkylsulfonate and alkylsulfate anions. *J. Phys. Chem. B* **2008**, *112*, 5039–5046.

(14) Cornell, W. D.; Cieplak, P.; Bayly, C. I.; Gould, I. R.; Merz, K. M.; Fergusin, D. M.; Spellmeyer, D. C.; Fox, T.; Caldwell, J. W.; Kollman, P. A. A 2nd generation force-field for the simulation of proteins, nucleic-acids, and organic-molecules. *J. Am. Chem. Soc.* **1995**, *117*, 5179–5197.

(15) Frisch, M. J.; Trucks, G. W.; Schlegel, H. B.; Scuseria, G. E.; Robb, M. A.; Cheeseman, J. R.; Montgomery, J. A., Jr.; Vreven, T.; Kudin, K. N.; Burant, J. C.; Millam, J. M.; Iyengar, S. S.; Tomasi, J.; Barone, V.; Mennucci, B.; Cossi, M.; Scalmani, G.; Rega, N.; Petersson, G. A.; Nakatsuji, H.; Hada, M.; Ehara, M.; Toyota, K.; Fukuda, R.; Hasegawa, J.; Ishida, M.; Nakajima, T.; Honda, Y.; Kitao, O.; Nakai, H.; Klene, M.; Li, X.; Knox, J. E.; Hratchian, H. P.; Cross, J. B.; Bakken, V.; Adamo, C.; Jaramillo, J.; Gomperts, R.; Stratmann, R. E.; Yazyev, O.; Austin, A. J.; Cammi, R.; Pomelli, C.; Ochterski, J. W.; Ayala, P. Y.; Morokuma, K.; Voth, G. A.; Salvador, P.; Dannenberg, J. J.; Zakrzewski, V. G.; Dapprich, S.; Daniels, A. D.; Strain, M. C.; Farkas, O.; Malick, D. K.; Rabuck, A. D.; Raghavachari, K.; Foresman, J. B.; Ortiz, J. V.; Cui, Q.; Baboul, A. G.; Clifford, S.; Cioslowski, J.; Stefanov, B. B.; Liu, G.; Liashenko, A.; Piskorz, P.; Komaromi, I.; Martin, R. L.; Fox, D. J.; Keith, T.; Al-Laham, M. A.; Peng, C. Y.; Nanayakkara, A.; Challacombe, M.; Gill, P. M. W.; Johnson, B.; Chen, W.; Wong, M. W.; Gonzalez, C.; Pople, J. A. *Gaussian 03*, revision C.05; Gaussian, Inc.: Wallingford, CT, 2004.

(16) Smith, W.; Forester, T. R. *The DL_POLY package of molecular simulation routines*, Version 2.13; The Council for the Central Laboratory of Research Councils, Daresbury Laboratory: Warrington, U.K., 1999.

(17) Renon, H.; Prausnitz, J. M. Local compositions in thermodynamic excess functions for liquid mixtures. *AIChE J.* **1968**, *14*, 135–144.

(18) Ott, J. B.; Holscher, I. F.; Schneider, G. M. (Liquid + liquid) phase-equilibria in (methanol + heptane) and (methanol + octane) at pressures from 0.1 to 150 MPa. *J. Chem. Thermodyn.* **1986**, *18*, 815–826.

(19) Najdanovic-Visak, V.; Esperança, J. M. S. S.; Rebelo, L. P. N.; Nunes da Ponte, M.; Guedes, H. J. R.; Seddon, K. R.; de Sousa, H. C.; Szydłowski, J. Pressure, Isotope, and Water Co-solvent Effects in Liquid-Liquid Equilibria of (Ionic Liquid + Alcohol) Systems. *J. Phys. Chem. B* **2003**, *107*, 12797–12807.

(20) Rebelo, L. P. N.; Sousa, H. C. A continuous polydisperse thermodynamic algorithm for a modified Flory-Huggins model. The (polystyrene+nitroethane) example. *J. Polym. Sci. B: Polym. Phys.* **2000**, *38*, 632–651.

(21) Hayman, H. J.; Eliezer, I. Dipole moments of alpha, omega-dibromoparaffins and their temperature dependence. *J. Chem. Phys.* **1961**, *35*, 644–648.

(22) McClelland, A. L. *Tables of Experimental Dipole Moments*; Freeman: San Francisco, CA, 1963.

(23) Nakamura, N.; Kamitake, Y. Dipole-moments of alpha, omega-dibromoalkanes. *Colloid Polym. Sci.* **1985**, *263*, 475–477.

(24) Thorbjornsrud, J.; Ellestad, O. H.; Klaboe, P.; Torgrimsen, T. Substituted propanes. 6. Vibrational-spectra and conformations of 1,3-dichloropropane, 1,3-bromochloropropane, 1,3-dibromopropane and 1,3-diiodopropane. *J. Mol. Struct.* **1973**, *15*, 61–76.

(25) Aroney, M.; Lefevre, J. W.; Izsak, D. Molecular polarisability - dipole moments, molar kerr constants, and apparent conformations of some alpha-omega-dichloro-alkanes and -dibromoalkanes. *J. Chem. Soc.* **1962**, 1407.

(26) Canongia Lopes, J. N.; Pádua, A. A. H. Nanostructural organization in ionic liquids. *J. Phys. Chem. B* **2006**, *110*, 3330–3335.

(27) Canongia Lopes, J. N.; Costa Gomes, M. F.; Pádua, A. A. H. Nonpolar, polar, and associating solutes in ionic liquids. *J. Phys. Chem. B* **2006**, *110*, 16816–16818.

(28) Rebelo, L. P. N.; Canongia Lopes, J. N.; Esperança, J. M. S. S.; Guedes, H. J. R.; Łachwa, J.; Najdanovic-Visak, V.; Visak, Z. P. Accounting for the unique, doubly dual nature of ionic liquids from a molecular thermodynamic and modeling standpoint. *Acc. Chem. Res.* **2007**, *40*, 1114–1121.

(29) Łachwa, J.; Szydłowski, J.; Makowska, A.; Seddon, K. R.; Esperança, J. M. S. S.; Guedes, H. J. R.; Rebelo, L. P. N. Changing from an unusual high-temperature demixing to a UCST-type in mixtures of 1-alkyl-3-methylimidazolium bis {(trifluoromethyl) sulfonyl}amide and arenes. *Green Chem* **2006**, *8*, 262–267.

(30) Shimizu, K.; Costa Gomes, M. F.; Pádua, A. A. H.; Rebelo, L. P. N.; Canongia Lopes, J. N. On the Role of the Dipole and Quadrupole Moments of Aromatic Compounds in the Solvation by Ionic Liquids. *J. Phys. Chem. B* **2009**, *113*, 9894–9900.

(31) LaPlante, A. J.; Stidham, H. D. Vibrational spectrum, ab initio calculations, conformational stabilities and assignment of fundamentals of 1,2-dibromopropane. *Spectrochim. Acta A* **2009**, *74*, 808–818.

(32) Oriani, R. A.; Smyth, C. P. Dipole moment and restricted rotation in some chlorinated hydrocarbons. *J. Chem. Phys.* **1949**, *17*, 1174–1178.

JP1025015